Journal of Crystal Growth 51 (1981) 336–344

LIQUID PHASE EPITAXY OF HEAVILY Te DOPED $Ga_{1-x}Al_xSb$ ON GaSB

P. GAUTIER, A. JOULLIÉ and G. BOUGNOT

Centre d'Etudes d'Electronique des Solides, associé au CNRS (LA 21), Université des Sciences et Techniques du Languedoc, Place E. Bataillon, F-34060 Montpellier Cédex, France

and

C.H. CHAMPNESS

Department of Electrical Engineering McGill University, 3480 University Street, Montreal, P.Q., Canada, H3A 2A7

Received 5 February 1980; manuscript received in final form 30 June 1980

Heavily tellurium doped $Ga_{1-x}Al_xSb$ alloys were grown by liquid phase epitaxy on p-GaSb undoped substrates. For high Te content liquid solutions ($X^L_{Te} \leq 0.5$ at%), quaternary $Ga_{1-x}Al_xSb_{1-y}Te_y$ solid solutions were deposited, with Y concentrations up to 0.23 near the substrate–alloy interface. The effective segregation coefficient of tellurium was found to be $k_{eff} = 23$ at 500°C and $k_{eff} = 12$ at 550°C. An n-type conductivity was observed with an upper electron density $n = 3 \times 10^{18}$ cm^{-3}. Measurements of the electron beam induced current by SEM have shown that the n–p junctions were situated at the chemical interface, with hole diffusion lengths of about 1 μm, and electron diffusion lengths of about 2 μm.

1. Introduction

The $Ga_{1-x}Al_xSb$ solid solution has been grown by zone melting [1–4], horizontal normal freezing [4], Bridgman growth [5], liquid phase epitaxy [6–22], and chemical vapor deposition [23]. This alloy appears very attractive for application in optoelectronic devices [10], as selective 1.06 μm photodetector [24], high speed avalanche photodiode [25,26] or solar cell [27].

The undoped solid solution is a p-type semiconductor. The n–p junctions have been prepared by liquid phase epitaxy using tellurium doping, with electron concentration less than 10^{18} cm^{-3}. Some electrical and photoelectrical properties of n–p $Ga_{1-x}Al_xSb$–GaSb [8,15,19] or $Ga_{1-x_2}Al_{x_2}Sb$–$Ga_{1-x_1}Al_{x_1}Sb$ [16–18,27] heterojunctions have been studied.

In this paper, we present our results on the liquid phase epitaxy of heavily Te doped $Ga_{1-x}Al_xSb$ from gallium rich liquid solution onto p-GaSb substrates. A nearly equilibrium growth method was used. The variations of the layer composition along the growth axis were studied by electron microprobe analysis, as the segregation of Te between the liquid and solid phases. For the highest values of the liquid Te concentrations (0.5 at%), an n-type quaternary $Ga_{1-x}Al_xSb_{1-y}Te_y$ solid solution was deposited. Some electrical characteristics of the epilayers are presented.

2. Experimental

2.1. Growth procedure

Epilayers have been grown on single crystals ⟨111⟩B undoped p-type GaSb substrates ($p = (1–2) \times 10^{17}$ cm^{-3}). A conventional sliding graphite boat in a horizontal quartz reactor tube in a pure hydrogen atmosphere was used. The GaSb substrates were prepared for growth by a 1 μm mechanical polishing followed by a 1.5% bromine–methanol etch just prior to insertion into the furnace. The lightly unsaturated solution was initially prepared with 6-9's Ga and Al elements and GaSb crystals. The tellurium

was added under the form of a 6-9's element, or with the aid of Te doped GaSb crystals ($n = 10^{18}$ cm^{-3}) when a layer doping level of less than 10^{18} cm^{-3} was required. A graphite piston under a quartz rod kept up the flatness of the liquid solution of 3 mm height and prevented any Sb or Te loss during the heat treatment. After the melt was kept at 550°C for an hour, it was brought into contact with the polished ⟨111⟩B surface of a GaSb source, held in the horizontal graphite drawer just before the GaSb substrate. The immersion time was 40 min. With these conditions, the melt was supposed to be very slightly supersaturated, when the GaSb source was slowly but continuously dissolved in the melt [28]. At this time the system was cooled, and then the source was retracted and replaced by the GaSb substrate. The growth was initiated on the substrate for various values of supercooling Δ (0–5°C) and cooling rate R (0.025, 0.66 and 2.25°C min^{-1}). As the first layers were deposited on the GaSb source, the growth on the substrate was very near the equilibrium.

2.2. Composition profiles

The solid compositions were determined using quantitative electron microprobe analysis; by comparison of the emission intensity of the Ga Kα, Al Kα Sb Lα and Te Lα radiations of the layer, with the emission intensity of Al, GaSb and GaTe check samples. The real concentrations were calculated using a correcting program taking into account backscattering, absorption and fluorescence effects [29].

The layers uniformity normal to the growth axis was controlled to be better than the accuracy of the microprobe analysis (±2 absolute at%).

The variations of the solid composition were studied normal to the substrate. The Te profiles were obtained by recording the signal of the Te Lα radiation. Tellurium concentration of 3×10^{-4} at. fraction could be detected in the solid phase.

3. Results

3.1. Layer morphology

Epilayers of 50-80 μm thickness were obtained for growth intervals varying from 15°C ($\Delta = 5$°C) to 20°C ($\Delta = 0$°C). The efficiency of the LPE experiments, calculated from the Ga–Al–Sb phase diagram [28], was about 20%. The as-grown surface was determined to be dependent of the substrate orientation. The ⟨111⟩B surfaces currently showed many ripples or triangular facets. Shining smooth surfaces were

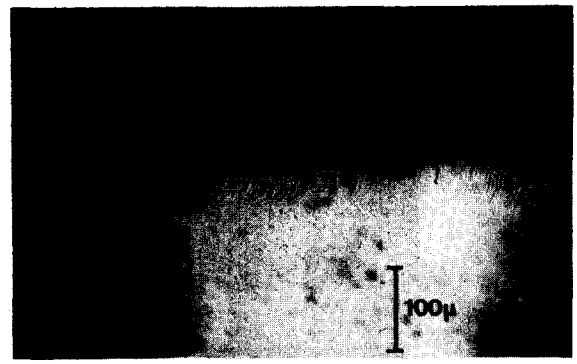

Fig. 1. (110) Cleavage plane of an epitaxial layer of Te doped $Ga_{0.60}Al_{0.40}Sb$ on (111)B GaSb substrate; growth conditions: $X^L_{Te} = 7.5 \times 10^{-5}$ at.fr.; $\Delta = 5$°C; $R = 2.25$°C mm^{-1}; growth interval 495–480°C.

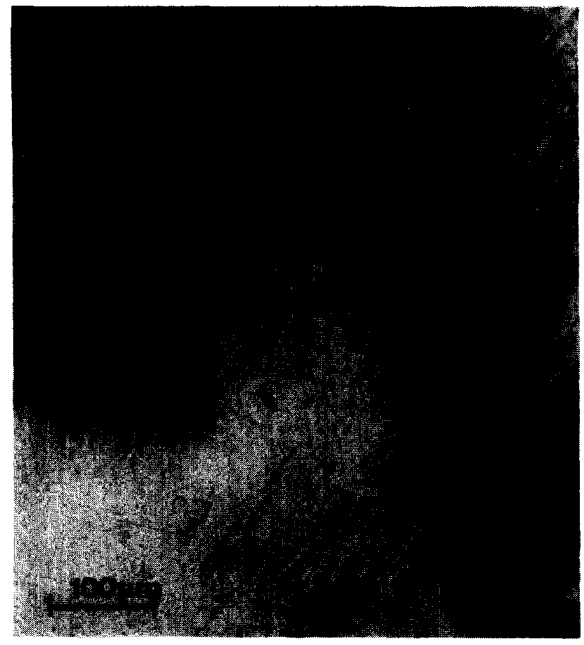

Fig. 2. (111)B surface of a $Ga_{0.60}Al_{0.40}Sb$ epilayer showing stacking faults.

Fig. 3. Dislocation loops chemically revealed by 1 HNO_3, 1 H_2O_2, 1 H_2O on a $Ga_{1-x}Al_xSb_{1-y}Te_y$–GaSb structure (X = 0.27); Y = 0.23 at the interface and 0.02 near the surface.

Fig. 4. Cracks and large striations parallel to the interface attributed to compositional Te variations revealed by 1 HNO_3, 1 HF, 1 H_2O on the same $Ga_{1-y}Al_xSb_{1-y}Te_y$–GaSb structure as presented in fig. 3.

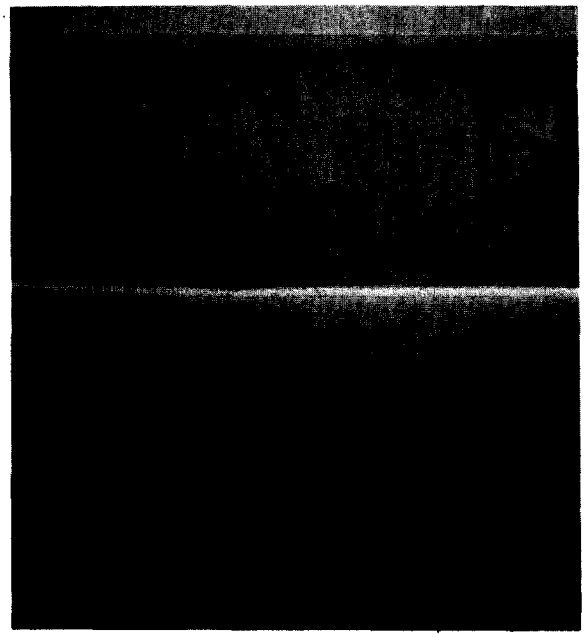

Fig. 5. p–n Junction of a $Ga_{1-x}Al_xSb_{1-y}Te_y$–GaSb structure visualized by EBIC in a SEM. The junction lies at the substrate–deposit interface.

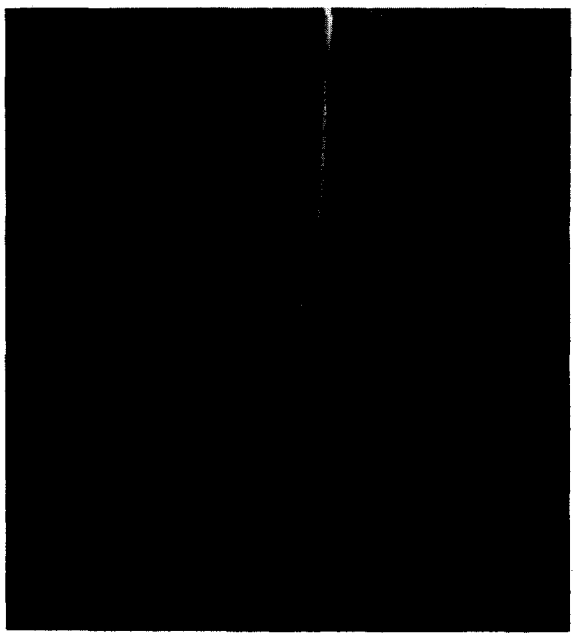

Fig. 6. Electron beam induced current across the same cleavage of fig. 5.

obtained only with ⟨111⟩B substrates perfectly oriented. On these surfaces, some stacking faults appear clearly. Other classical orientations were not selected for this study, as they appeared less favourable for the LPE growth: ⟨111⟩A surfaces showed hillocks and spiral growth patterns, and ⟨100⟩ surfaces were cellular.

The substrate was strongly dissolved with $\Delta = 0$ and slow deposition rates. This dissolution was reduced until a few microns using $\Delta = 5°C$ and highest cooling rates. Linear layer–substrate interfaces free of solvent inclusions were obtained if the seed orientation was off by less than about 1/2° and for high tellurium concentration in the liquid. It has been shown that misoriented substrates give a stepped etch back [30]. The favourable influence of tellurium upon the linearity of the interface, observed for other LPE experiments [31], could not been explained.

Typical cleavages of the structure and as-grown surfaces are shown in figs. 1 and 2. Some defects revealed by chemical etching normal to the substrate are presented in figs. 3 and 4.

The position of the n–p junctions and the diffusion length of the minority carriers were determined from the current induced by the electron beam of a SEM. As shown in the fig. 5, the n–p junction revealed by scanning lays at the substrate–deposite interface. Hole diffusion lengths of about 1 μm were measured from the drop of the induced current profile (fig. 6). Electron diffusion lengths in the substrare are 1–2 μm.

3.2. Composition profiles

Fig. 7 shows the recorded concentration profiles of tellurium in epilayers of Al composition $X \sim 0.20$, for various Te liquid concentrations X^L_{Te}. A great quantity of tellurium was found in the deposite. A sharp increase of the Te profile was noted near the substrate–alloy interface for layers grown with $X^L_{Te} = 5 \times 10^{-3}$ at.fr. The Te peak value is $\gtrsim$10 at%. This peak becomes weaker as X^L_{Te} decreases. For the lowest values of X^L_{Te}, the distribution of Te through the layer seems to be uniform, but in this case the microprobe sensitivity (300 atppm) is of the same order of magnitude as the measurement (300 to 1000 atppm).

Quantitative measurements of the composition of

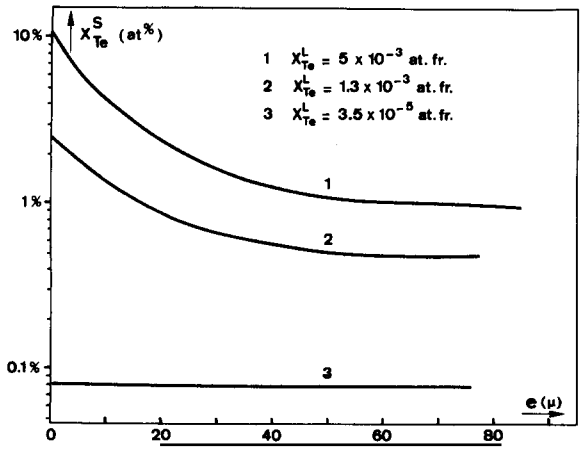

Fig. 7. Tellurium concentration profiles in epilayers grown at 500–480°C from liquids of different Te concentrations.

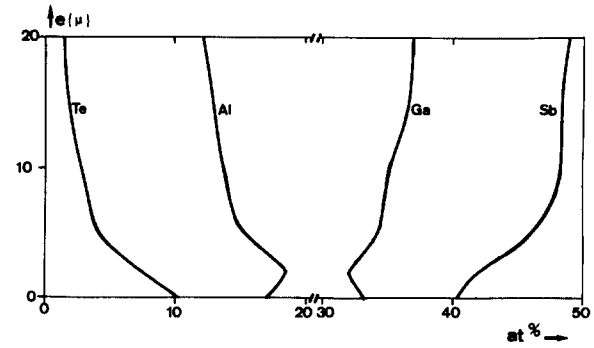

Fig. 8. Quantitative electron microprobe analysis of the four elements on a cross section of the epilayer.

the whole solid phase were made in several points of the layers. Results are indicated in fig. 8 for a layer grown from a liquid of tellurium concentration $X^L_{Te} = 5 \times 10^{-3}$ at.fr. It can be seen that in all cases:

$$X^S_{Ga} + X^S_{Al} \sim X^S_{Sb} + X^S_{Te} \sim 0.5 \text{ at.fr} .$$

So the deposit appears to be the quaternary solid solution $Ga_{1-x}Al_xSb_{1-y}Te_y$, where the tellurium atoms replace the antimony atoms on the B sublattice.

This result agrees with the reported works on the GaSbTe phase diagram, which indicate the existence of a GaSb–GaTe solid solution up to 16.4 mol% GaTe [32,33].

The value of X was determined from the ratio of the calculated atomic concentrations of Ga and Al in the layers. The variations of X along the growth axis are reported in fig. 9. They are compared with the theoretical previsions made from the knowledge of the ternary Ga–Al–Sb phase diagram [28]. The

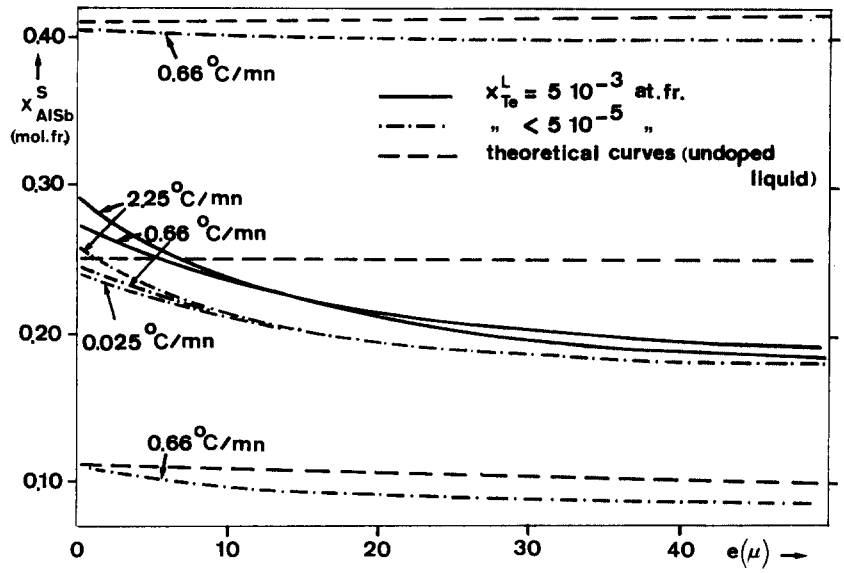

Fig. 9. Aluminum concentration profiles of epitaxial layers on GaSb substrates.

influence of R and X^L_{Te} was studied for layers grown from a liquid containing one percent of aluminium.

The theoretical predictions give a homogeneous alloy in the whole range of growth. This is not the case here. The Al concentration decreases within a thickness of 20–30 μm and remains under the equilibrium value. The slope of the profile is more pronounced when the cooling rate increases. Such behaviour was noted in the LPE of $Ga_xIn_{1-x}Sb$ [34]. It can be explained by the formation of a solute depletion layer which takes place near the solid–liquid interface [35,36].

For epilayers grown from a lightly Te doped liquid solution, the X value of the first deposite crystals is predicted by the ternary Ga–Al–Sb phase diagram. This composition is higher for strongly tellurium doped liquids. In this case the liquid concentration of tellurium cannot be neglected. It has been shown that the 536°C liquidus isotherm of the Ga–Al–Sb ternary diagram is slightly displaced up to higher Sb liquid concentrations when the melt is doped with 0.04 at% tellurium [18]. So, for highly Te doped liquids, the quaternary Ga–Al–Sb–Te phase diagram must govern the solid phase composition, as its evolution during the cooling.

3.3. Tellurium segregation

The effective segregation coefficient of tellurium was defined as:

$$k^{Te}_{eff} = X^S_{0,Te}/X^L_{Te},$$

where $X^S_{0,Te}$ is the tellurium atomic concentration in the first deposite which was determined by microprobe analysis. Fig. 10 shows the values of k^{Te}_{eff} versus X^L_{Te} for layers of $X = 0.20$ grown at 500 and 550°C. The value of k^{Te}_{eff} was found to be independent of X^L_{Te} in the studied liquid composition range: $k^{Te}_{eff} = 23$ at 500°C and 12 at 550°C. These values have the same order of magnitude as the distribution coefficients of Al and Sb calculated in the same manner (table 1). For melt growth at 750°C of $Ga_{0.70}Al_{0.30}Sb$ crystals, k^{Te}_{eff} was determined to be equal to 0.7 [5]. So k^{Te}_{eff} (as k^{Sb}_{eff}) is strongly reduced when the growth temperature is increased.

3.4. Electrical data

The electrical properties of the layers were studied by Hall effect and resistivity measurements after lapping the GaSb substrate and the inhomogeneous part of the deposite near the substrate. The material conductivity was n-type. The variations of the carrier concentration ($n = 1/R_H e$) and electron mobility ($\mu = R_H/\rho$) versus X^L_{Te} are shown in the fig. 11. The values of n determined from C–V measurements by Anderson et al [14] on $Ga_{0.45}Al_{0.55}$ Sb samples grown at 500°C are also reported, with the Te concentration N_D(atoms cm^{-3}) calculated from the knowledge of k^{Te}_{eff} and taking the obtained interface value as bulk value (this assumption appears reasonable for $X^L_{Te} < 10^{-4}$ at.fr) Fig. 11 shows that for $X^L_{Te} < 3.10^{-6}$ at.fr., $n \sim N_D$. Each atom of tellurium furnishes a conduction electron. For $X^L_{Te} > 3 \times 10^{-6}$

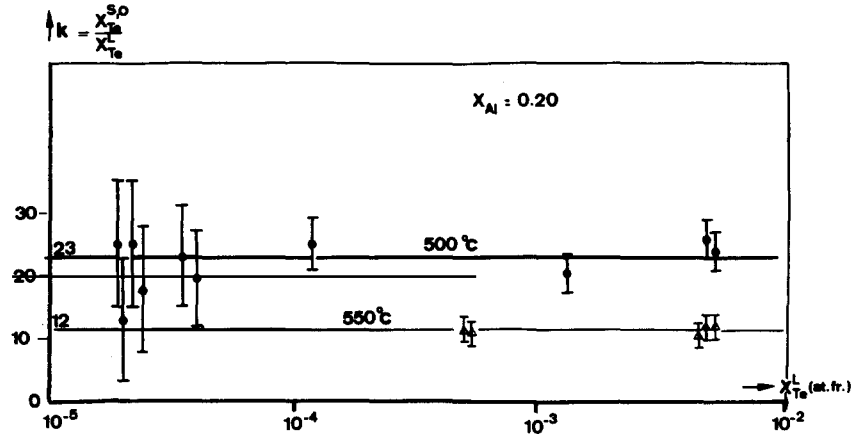

Fig. 10. Tellurium segregation coefficient $k = X^S_{0,Te}/X^L_{Te}$ as a function of the Te concentration of the initial liquid X^L_{Te}.

Table 1
Measured effective segregation coefficients of Al, Sb and Te in the LPE and melt growth of $Ga_{1-x}Al_xSb_{1-y}Te_y$

Saturation temperature (°C)	X^L_{Al} (at.fr.)	X^L_{Te} (at.fr.)	k^{Al}_{eff}	k^{Sb}_{eff}	k^{Te}_{eff}	X	Y
500	0.01	0	12	22	23	0.24	0
500	0.01	0.005	14	17	23	0.28	0.23
550	0.01	0.005	10	9	12	0.20	0.12
750 (from ref. [5])	0.02	0.001	7.5	1	0.7	0.30	

The variations of X^L_{Al} and X^L_{Te} resulting from the GaSb charge dissolution were neglected. k^{Sb}_{eff} was estimated taking the equilibrium values of X^L_{Sb} furnished by the Ga–Al–Sb ternary diagram [28], neglecting the influence of tellurium upon the liquidus isotherm.

at.fr., the carrier concentration tends to an upper limit of about 3×10^{18} cm^{-3}.

The limit of the effective number of tellurium donors may be the occurrence of a compensating mechanism due to p-type impurities (like Cu–0) or lattice vacancies.

The carrier concentration of undoped $Ga_{1-x}Al_xSb$ grown by LPE in our experiments was $p = 8-10 \times 10^{16}$ cm^{-3}. This residual concentration is relatively high and can be attributed to an off-stoichiometry defect like in GaSb [40] or GaInSb [41]. But it remains too low to compensate Te donors near 10^{18} cm^{-3}.

It has been shown in GaSb doped with tellurium that lattice vacancies tend to develop on the A sublattice as the concentration of Te is increased [37]. But this mechanism is regular and cannot explain the sudden drop of the electron mobility to very low values as $X^L_{Te} > 10^{-5}$ at.fr. (fig. 11).

This drop can coincide with the appearance of a second phase as observed by Hall and Racette [38] on heavily doped GaSb crystals although chemical

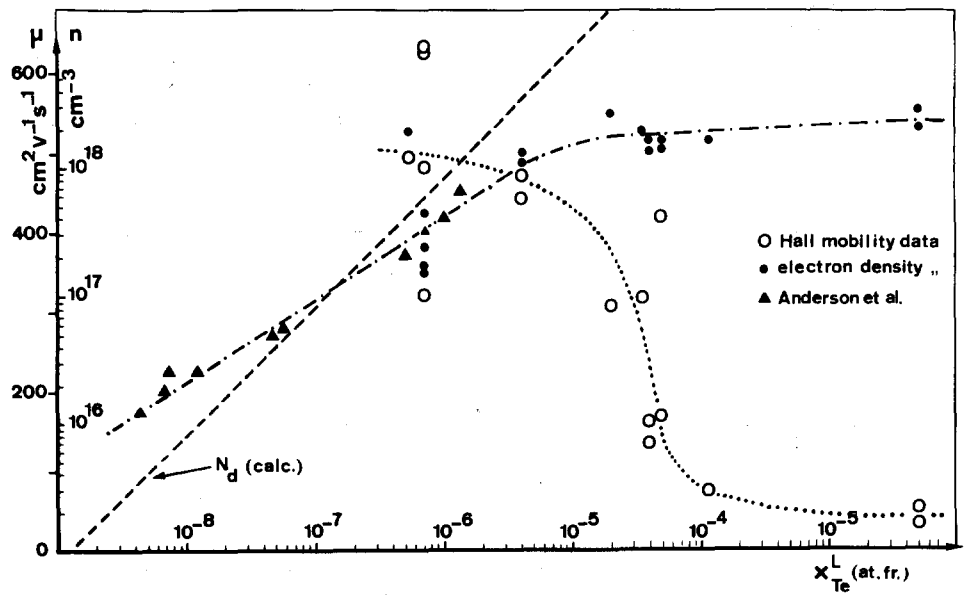

Fig. 11. Electrical characteristics of Te doped $Ga_{1-x}Al_xSb$ LPE layers (X = 0.20–0.30) grown at 500°C.

etching of the layers did not show any local inhomogeneity of composition, as X-ray recording of Te by Castaing microprobe.

A study of the surface structure of an undoped GaSb substrate and a Te doped epilayer ($n = 2.5 \times 10^{18}$ cm^{-3} corresponding to $X^L_{Te} = 1.3 \times 10^{-3}$ at.fr) was made by scanning ellipsometry measurements using a 5 μm luminous spot and a wavelength of 6328 Å [39]. The fluctuations of the ellipsometry data across the scanned surface (1×1 mm^2) were similar for the two samples (about 1%).

These experiments show that if the layer does not remain single phase with high tellurium concentrations, the second phase which would be formed must appear in the form of nuclei of small dimensions (less than 5 μm) and regularly shared into the solid.

4. Conclusion

$Ga_{1-x}Al_xSb_{1-y}Te_y$ solid solutions were obtained at 500°C from liquids with tellurium concentrations $X^L_{Te} \leqslant 5 \times 10^{-3}$ at.fr. The 500°C effective segregation coefficient of Te was found to be $k^{Te}_{eff} = 23$. Its value decreases when the growth temperature is raised. The Te repartition into the layer was inhomogeneous. Melts with $X^L_{Te} = 5 \times 10^{-3}$ at.fr. give $Y \sim 0.2$ near the interface and $Y \sim 0.01$ near the surface of the deposite.

The epilayers were n-type with a limit for the electron concentration of 3×10^{18} cm^{-3}. The drop of the mobility as $X^L_{Te} > 10^{-5}$ at.fr. can be explained by the appearance of a second phase, but this phase could not be detected in our experiments.

Acknowledgements

The authors wish to thank J.P. Roux for his help in the LPE experiments, A. Gouskov for the GaSb Czochralsky ingots supplying, and J.F. Bresse, R. Aulombard and S. Gaillard for respectively the EBIC, Hall effect and ellipsometry measurements.

References

[1] N.A. Goryunova and I.I. Burdiyan, Dokl. Akad. Nauk SSSR 120 (1958) 1031.
[2] I.I. Burdiyan and A.S. Borschevskii, Zh. Tekhn. Fiz. 28 (1958) 2684.
[3] A.S. Borschevskii, I.I. Burdiyan, Yu. Lubenskaya and E.V. Sokolova, Russ. J. Inorg. Chem. 4 (1959) 1306.
[4] J.F. Miller, H.L. Goering and R.C. Himes, J. Electrochem. Soc. 107 (1960) 527.
[5] R.L. Aulombard and A. Joullié, Mater. Res. Bull. 14 (1979) 349.
[6] T.S. Gontcharova, S.G. Koniikov, N.G. Riabtsev, D.N. Tret'yakov and T.P. Alexandrovna, Izv. Vyssh. Ucheb. Zaved. Fiz. 16 (1973) 146.
[7] L.V. Golubev, O.A. Khachaturyan, A. Ya. Shik and Yu.V. Shmartsev, Phys. Status Solidi (a) 22 (1975) 1150.
[8] V.P. Germogenov, A.A. Vilisov and A.P. Vyatkin, Izv. Vyssh. Uchebn. Zaved Fiz. 18 (1975) 63.
[9] S.M. Bedair, J. Electrochem. Soc. 122 (1975) 1150; J. Appl. Phys. 47 (1976) 4145.
[10] K.Y. Cheng, Technical Report No. 5111-5, Stanford, August 1975.
[11] A. Nguyen Van Mau, C. Ance and G. Bougnot, J. Crystal Growth 36 (1976) 273.
[12] V.A. Gevorkyan, L.V. Golubev, S.G. Petrosyan, A.Ya. Shik and Yu. Shmartsev, Soviet Phys.- Tech. Phys. 22 (1977) 750.
[13] K.Y. Cheng and G.L. Pearson, J. Electrochem. Soc. 124 (1977) 753.
[14] S.J. Anderson, F. School and J.S. Harris, in: Proc. 6th Intern. Conf. on GaAs and Related Compounds, St. Louis, 1976 (Inst. Phys. Conf. Ser. No. 33b, 1977) p. 346.
[15] N.S. Simogorova, S.G. Konnikov, I.I. Matkova and D.N. Tret'yakov, Soviet Phys.-Semicond. 10 (1976) 399.
[16] A.N. Imenkov, T.P. Lideikis, B.V. Tsarenkov, Yu.M. Shernyakov and Yu.P. Yakovlev, Soviet Phys.-Semicond. 10 (1976) 748.
[17] T.T. Dedegkaev, A.N. Imenkov, I.I. Kryukov, T.P. Lideikis B.V. Tsarenkov, Yu.M. Shernyakov and Yu. Yakovlev, Soviet Phys.-Semicond. 11 (1977) 155.
[18] Y. Muoy, Thesis, Montpellier University (1977).
[19] T. Sukegawa, T. Hiraguchi, A. Tanaka and M. Hagino, Appl. Phys. Letters 32 (1978) 376.
[20] T.T. Dedegkaev, I.I. Kryukov, T.P. Lideikis, B.V. Tsarenkov and Yu. Yakovlev, Soviet Phys.-Tech. Phys. 23 (1978) 350.
[21] G. Motosugi and T. Kagawa, Japan. J. Appl. Phys. 17 (1978) 2061.
[22] R. Linnebach, Thesis, Stuttgart University (1978).
[23] N. Kitamura, M. Kakehi and T. Wada, J. Crystal Growth 45 (1978) 176.
[24] Z.I. Alferov, N.S. Simogorova, S.G. Konnikov, I.I. Matkova L. Tramatarova and D.N. Tret'yakov, Pis'ma Zh. Tekh. Fiz. 1 (1975) 641.
[25] H.D. Law, R. Nakano, L.R. Tomasetta and J.S. Harris, Appl. Phys. Letters 33 (1978) 948.
[26] B. Tomasetta, H.D. Law and K. Nakano, Laser Focus (Dec. 1978) 42.

[27] A. Nguyen van Mau, G. Bougnot, H.Y. Muoy and G.M. Moussali, Photovoltaic Solar Energy Conf., Luxembourg, 1977.
[28] A. Joullie, P. Gautier and E. Monteil, J. Crystal Growth 47 (1979) 100.
[29] J.W. Colby, in: Proc. 6th Natl. Conf. on Electron Probe Analysis, Pittsburgh, Pennsylvania, EPASA 17A-17B, 1971.
[30] R.H. Saul and D.D. Roccasecca, J. Appl. Phys. 44 (1973) 1983.
[31] T. Tamura, T. Moriizumi and K. Takahashi, Japan, J. Appl. Phys. 11 (1972) 1024.
[32] M.S. Mirgalovskaya and E.M. Komova, Vopr. Met. i. Fiz. Poluprov. Akad. Nauk. SSR, Trudy 4-go Soveshch, Moscow 138-44, 1961 (Proc. 4th All-Union Conf. on Semiconductor Materials, Ed. N.Kh. Abrikosov (Consultants Bureau, New York, 1963)).
[33] N.A. Goryunova, A.A. Aborukhmanova and M.I. Aliev, Dokl. Akad. Nauk Azerb. SSR 21 (1965) 13.
[34] A. Joullié, R. Aulombard and G. Bougnot, J. Crystal Growth 24/25 (1974) 276.
[35] J. Crossley and M.B. Small, J. Crystal Growth 15 (1972) 268.
[36] A. Joullié, J. Crystal Growth 38 (1977) 45.
[37] J.C. Woolley and K.W. Blazey, J. Electrochem. Soc. 111 (1964) 951.
[38] R.N. Hall and J.H. Racette, J. Appl. Phys. 32 (1961) 856.
[39] Scanned ellipsometry technics were developed in the Lab. d'Optique, USTL, Montpellier, France, by C. Alibert and S. Gaillard.
[40] R.D. Baxter, R.T. Bate and F.J. Reid, J. Phys. Chem. Solids 28 (1965) 41.
[41] J. Allegre, M. Averous, R. Jourdan et A. Joullié, J. Luminescence 11 (1976) 339.